Published in final edited form as:
J Struct Biol. 2013 February ; 181(2): 185–189. doi:10.1016/j.jsb.2012.11.001.

Crystal Structures of Acetate Kinases from the Eukaryotic Pathogens *Entamoeba histolytica* and *Cryptococcus neoformans*

Tarjani M. Thaker[a], **Mikio Tanabe**[b,@], **Matthew L. Fowler**[c], **Anita M. Preininger**[b], **Cheryl Ingram-Smith**[c], **Kerry S. Smith**[c], and **T.M. Iverson**[a,b,*]

[a]Department of Biochemistry Vanderbilt University Medical Center, Nashville, TN, 37232, USA

[b]Department of Pharmacology, Vanderbilt University Medical Center, Nashville, TN, 37232, USA

[c]Departments of Genetics and Biochemistry, Clemson University, Clemson, SC, 29634, USA

Abstract

Acetate kinases (ACKs) are members of the acetate and sugar kinase/hsp70/actin (ASKHA) superfamily and catalyze the reversible phosphorylation of acetate, with ADP/ATP the most common phosphoryl acceptor/donor. While prokaryotic ACKs have been the subject of extensive biochemical and structural characterization, there is a comparative paucity of information on eukaryotic ACKs, and prior to this report, no structure of an ACK of eukaryotic origin was available. We determined the structures of ACKs from the eukaryotic pathogens *Entamoeba histolytica* and *Cryptococcus neoformans*. Each active site is located at an interdomain interface, and the acetate and phosphate binding pockets display sequence and structural conservation with their prokaryotic counterparts. Interestingly, the *E. histolytica* ACK has previously been shown to be pyrophosphate (PP_i)-dependent, and is the first ACK demonstrated to have this property. Examination of its structure demonstrates how subtle amino acid substitutions within the active site have converted cosubstrate specificity from ATP to PP_i while retaining a similar backbone conformation. Differences in the angle between domains surrounding the active site suggest that interdomain movement may accompany catalysis. Taken together, these structures are consistent with the eukaryotic ACKs following a similar reaction mechanism as is proposed for the prokaryotic homologs.

Keywords

Acetate kinase; PP_i-dependent kinase; ASKHA superfamily

1. Introduction to acetate kinases

Enzyme-catalyzed phosphoryl transfer reactions are important for a range of biological activities. Acetate kinases (ACKs) transfer a phosphoryl group to and from acetate, thus

*Corresponding author. 460 Robinson Research Building, 23rd Ave. South at Pierce, Vanderbilt University Medical Center, Nashville, TN 37232-6600. tina.iverson@vanderbilt.edu. Phone: 615-322-7817. Fax: 615-343-6532.
@Present address: HALOmem, Institut für Biochemie und Biotechnologie, Martin-Luther-Universität Halle–Wittenberg, 06120 Halle (Saale), Germany

promoting the interconversion of acetate and acetyl phosphate. With this transformation, ACKs play a role in multiple, distinct bioenergetic pathways (Cozzone, 1998; Ingram-Smith et al., 2006; Thauer et al., 2008). For example, in fermentative bacteria, the ACK-catalyzed dephosphorylation of acetyl phosphate has been demonstrated to be essential for the ACK-phosphotransacetylase (ACK-PTA) bioenergetic pathway, which utilizes energy stored in acetyl-CoA (Cozzone, 1998). Similarly, ACK-dependent dephosphorylation of acetyl phosphate facilitates ATP synthesis via the pentose phosphoketolase pathway in fungi (Ingram-Smith et al., 2006). Conversely, in the methanoarchaeon *Methanosarcina*, ACK activates acetate for its conversion to acetyl-CoA in the first step of acetioclastic methanogenesis (Thauer et al., 2008). While the investigations into ACK enzymes have focused on bacterial and archaeal systems, ACK was identified in the eukaroyote *Entamoeba histolytica* in the early 1960s (Bragg and Reeves, 1962) and was first biochemically characterized in the 1970s (Reeves and Guthrie, 1975). Genes encoding putative ACKs have since been identified within the genomes of other eukaryotic pathogens, including the basidomycete *Cryptococcus neoformans* (Ingram-Smith et al., 2006). At least in *E. histolytica*, the organism does not appear to have homologs for other proteins required for the known bioenergetic pathways that use ACK (Fowler et al., 2012). This suggests that the biological function of the *E. histolytica* ACK may be different from that demonstrated in prokaryotes, but at present, that function remains unknown.

ACKs belong to the acetate and sugar kinase/hsp70/actin (ASKHA) superfamily (Buss et al., 1997). Members of this family use tandem RNase-H like folds as a scaffold for the optimal positioning of five signature sequence motifs, three of which (termed ADENOSINE, PHOSPHATE 1, and PHOSPHATE 2) form the ATP binding pocket (Fig. 1A, B) (Hurley, 1996). While the oligomeric states of ASKHA superfamily members can differ, each protomer fully houses a complete active site.

Biochemical and structural investigations of ACK from the methanogenic archaeon *Methanosarcina thermophila* have been key in developing a mechanistic proposal for ACKs (Buss et al., 2001; Gorrell et al., 2005; Ingram-Smith et al., 2000; Miles et al., 2001; Miles et al., 2002; Singh-Wissmann et al., 2000). It is now generally accepted that phosphoryl transfer between the nucleotide and the substrate occurs directly via an in-line mechanism. This is supported by a crystal structure of the *M. thermophila* ACK in complex with acetate and the nucleotide transition state analog ADP-AlF_3 (Gorrell et al., 2005), which showed the two cosubstrates bound within the active site in a linear array. The structural evidence for the in-line transfer mechanism effectively ended a long-standing debate on the role of ACK phosphoenzyme, which had originally been proposed as a catalytic intermediate.

Domain motions are proposed to facilitate catalysis in *M. thermophila* ACK by closing around the cosubstrates, which correctly aligns the γ-phosphate of ATP (or pyrophosphate (PP_i)) with the phosphoryl acceptor (Gorrell et al., 2005). Fluorescence quenching experiments demonstrated that the differences in interdomain angle observed in the crystal structures of numerous ASKHA enzymes indeed convert to interdomain movement (Gorrell, 2007; Hurley, 1996).

Mirroring the state of knowledge on the biological function of eukaryotic ACKs, few direct studies on the enzymatic mechanism of eukaryotic enzymes have been performed and it is not clear how (or if) the mechanism is modified with respect to the mechanism proposed for the *M. thermophila* enzyme (Gorrell et al., 2005). Interestingly, the *E. histolytica* ACK has been shown to use P_i/PP_i, rather than ADP/ATP, as the phosphoryl acceptor/donor pair for phosphoryl transfer (Fowler et al., 2012; Reeves and Guthrie, 1975). Further, this enzyme has a strong kinetic advantage for catalyzing the dephosphorylation of acetyl phosphate (Fowler et al., 2012; Reeves and Guthrie, 1975). Although a kinetic characterization has not

yet been reported in the literature, *C. neoformans* ACK has also been shown to kinetically favor acetate formation (Ingram-Smith, C., personal communication). Here, we report the crystal structures of the *E. histolytica* and *C. neoformans* ACKs at 2.4 Å and 1.9 Å resolution, respectively. These provide a structural basis for catalysis in the eukaryotic ACKs.

2. Protein expression and purification

The *E. histolytica* ACK gene cloned into the pQE30 plasmid was co-transformed with the *lacI*-containing plasmid pREP-4 into *Escherichia coli* YBS121 (a generous gift of George Bennett, Rice University). The *C. neoformans* ACK gene was cloned into the pET21b plasmid and transformed into *E. coli* Rosetta2 (*DE3*). Both were expressed and purified using similar methods to those described for *E. histolytica* ACK (Fowler et al., 2012). Briefly, expression cultures were grown in LB broth containing the appropriate antibiotic at 37°C with shaking until the OD_{600} reached 0.9. Expression was induced with the addition of IPTG to a final concentration of 1 mM. Cultures were shaken overnight at ambient temperature.

Cells were harvested by centrifugation and resuspended in purification buffer (25 mM Tris, 150 mM NaCl, 20 mM imidazole, and 10% glycerol, pH 7.4). Cells were lysed using a French pressure cell and the cellular debris removed by centrifugation at 100,000 × g for 1 hour. ACK was purified from clarified lysate using a 5 mL HisTrap Ni-affinity column and eluted with a linear gradient from 20 mM to 500 mM imidazole in purification buffer. Each protein was pooled and dialyzed against buffer containing 25 mM Tris, 150 mM NaCl, and 10% glycerol, pH 7.4 and further purified by size exclusion chromatography using a Superdex S200 10/300GL column.

3. Crystallization, data collection, structure determination and refinement

E. histolytica ACK was crystallized using the hanging drop vapor diffusion method by mixing 1 μL protein (8 mg/mL in 25 mM HEPES, pH 7.5) with 1 μL reservoir solution (50 mM ADA, 0.6 M potassium-sodium tartrate, 10 mM $FeCl_3$, pH 6.6) and equilibrating against 1 mL reservoir solution at 20°C. Crystals formed within 3 days and were cryo-protected in a solution containing all of the crystallization components and 30% ethylene glycol prior to flash cooling in liquid nitrogen.

C. neoformans ACK was crystallized by the hanging drop vapor diffusion method by mixing 1 μL protein (3 mg/mL in 25 mM Tris, pH 7.4) with 1 μL reservoir solution (50 mM ADA, 100 mM sodium tartrate, 18.5% PEG 2000, pH 6.2) and equilibrated against 1 mL reservoir solution at 4°C for 4 days. Crystals were cryo-protected by soaking in a solution containing all of the components of the crystallization reaction, but with the PEG 2000 concentration increased to 30% and then flash cooled in liquid nitrogen.

Crystallographic data were collected at the Advanced Photon Source LS-CAT beamlines (Table 1) and processed using HKL2000 (Otwinowski and Minor, 1997). The structures of both eukaryotic ACKs were determined by molecular replacement using the program PHASER (McCoy et al., 2007) and a polyalanine model of the *M. thermophila* ACK structure (PDB entry 1G99; (Buss et al., 2001)) as the search model. Preliminary phases for the *C. neoformans* ACK model were calculated in DM (Cowtan, 1994) and improved by solvent-flattening and two-fold non-crystallographic symmetry (NCS) averaging. Manual model building was performed in COOT (Emsley and Cowtan, 2004) and refinement was performed in CNS (Brunger et al., 1998) and REFMAC (Murshudov et al., 1997). Tight NCS restraints applied to individual domains of the *C. neoformans* ACK model were

reduced as the model quality improved. Final model quality was assessed with PROCHECK (Laskowski et al., 1993). Figures were prepared with PyMOL (Schrodinger, 2010).

4. Overall structures

On a global level, the structures of both eukaryotic ACKs (Fig. 2A, B) are similar to that of the previously reported *M. thermophila* ACK. This dimer has been described as resembling a bird with wings spread (Buss et al., 2001). The 'body' of the bird contains the C-terminal RNase-H like domain and mediates dimerization, while the 'wing' is organized around the N-terminal RNase-H like domain.

Superposition of each protomer of the *E. histolytica* and *C. neoformans* ACKs revealed that while each domain is folded similarly, there is a difference in the interdomain angle between the body and wing domains. This gives rise to unique rotation axes that superimpose the body and wing domains in both structures (Fig 2A, B). The difference in angle was calculated using DynDom (Hayward and Lee, 2002) and revealed a difference in interdomain angle of 9° between the two protomers of *E. histolytica* ACK and 14° between the two protomers of the *C. neoformans* ACK.

5. Active site architecture

The *M. thermophila* ACK is the closest structurally characterized homolog of the eukaryotic ACKs, and will be used for comparisons in this report. Comparison of each eukaryotic ACK to *M. thermophila* ACK determined in the presence of acetate, ADP-AlF_3, and thiopyrophosphate (PPS) (Gorrell et al., 2005) supports the assignment of the active site at the interface of the body and wing domains and suggests a binding site for the phosphoryl donor (ATP or PP_i) and acetate. The three signature motifs that mediate ATP binding in the ASKHA superfamily, termed ADENOSINE, PHOSPHATE 1, and PHOSPHATE 2 (Bork et al., 1992), surround the putative phosphoryl donor binding pocket in both of the eukaryotic ACKs (Fig. 1A). Co-crystallization of the *E. histolytica* and *C. neoformans* ACKs with either PP_i or nucleotide analogs, respectively, did not result in the appearance of new electron density corresponding to a bound phosphoryl donor in this site. Instead, superpositions with the structure of acetate and ADP-AlF_3 bound *M. thermophila* ACK (Fig. 3A, D) were used to evaluate whether the phosphoryl donor could reasonably be accommodated in a similar location within the eukaryotic ACKs. Manual modeling of ADP-AlF_3 into the structure of the *C. neoformans* ACK (Fig. 3B, E) and PPS into the structure of the *E. histolytica* ACK (Fig. 3C, F) resulted in reasonable contacts between protein and the respective nucleotide analogs.

The ADENOSINE motif normally positions the protein side chains into conformations that promote the interaction between protein and the adenosine base of ATP in ASKHA superfamily enzymes (Bork et al., 1992). Interestingly, both the sequence and the backbone structure of the ADENOSINE motif are conserved in the *E. histolytica* ACK (Fig. 1A, 3F), which has been demonstrated to use PP_i, and not ATP, as a phosphoryl donor (Fowler et al., 2012). Inspection of the *E. histolytica* ACK structure shows that substitution of a conserved glycine to glutamine and isoleucine to methionine (Gln-323 and Met-324 on α2A′) sterically occludes the ATP-binding cleft (Fig. 3C, F). Additionally, a salt bridge between Asp-272 and Arg-274 on αg stabilizes an alternate conformation of Arg-274 which positions its guanidino group into the ATP-binding cleft further contributing to the occlusion. These features may be important in the conversion of phosphoryl donor selectivity from ATP to PP_i.

The structure of the *M. thermophila* ACK in complex with its substrate acetate (Fig. 3A, G) revealed a hydrophobic substrate-binding pocket between the wing and body domains

(Gorrell et al., 2005). Manual modeling of acetate into both the *C. neoformans* (Fig. 3B, H) and *E. histolytica* ACKs (Fig. 3C, I) again resulted in reasonable contacts between protein and substrate. Indeed, the residues surrounding the acetate-binding pocket are almost completely conserved in the eukaryotic ACKs with the exception of a proline to threonine substitution at position 223 in the *E. histolytica* enzyme (Fig. 3I). However, site-directed mutagenesis studies of Thr-223 in *E. histolytica* ACK did not reveal a specific role for this side chain (Fowler et al., 2012).

6. Mechanistic implications

Given the similarities observed within the active sites of the *M. thermophila*, *C. neoformans*, and *E. histolytica* ACKs, it is reasonable to use the mechanism proposed for the *M. thermophila* enzyme as a starting proposal for eukaryotic ACKs. Each of the enzymes has an active site that would support binding of the acetate and the phosphoryl donor (either ATP or PP_i) in a linear arrangement (Fig. 3A–C). This binding mode is consistent with the in-line transfer mechanism proposed for *M. thermophila* ACK, where the phosphoryl transfer occurs directly between the two properly aligned cosubstrates (Gorrell et al., 2005).

The biological role of ACK in *M. thermophila* is to produce acetyl phosphate (and ADP) from acetate and ATP during methanogenesis (Buss et al., 2001). The reaction is therefore commonly discussed in the acetyl phosphate forming direction, although *in vitro,* the *M. thermophila* enzyme catalyzes the reverse reaction at a similar rate (Miles et al., 2001; Fowler et al., 2012). In contrast, kinetic characterization of both the *E. histolytica* ACK (Fowler et al., 2012; Reeves and Guthrie, 1975) and the *C. neoformans* ACK (Ingram-Smith, C., personal communication) revealed faster turnover in the acetate-forming direction. It is unclear from the structures why the reaction is favored in one direction while the *M. thermophila* enzyme appears to catalyze the same reaction bidirectionally with comparable efficiency (Miles et al., 2001). Nevertheless, it is conceivable that the in-line transfer could work in reverse. In this scenario, acetyl phosphate and P_i/ADP would bind in a linear array within the active site, and the phosphoryl group would be transferred from the acetyl phosphate to the P_i/ADP.

The difference in interdomain angle observed in both the *E. histolytica* and *C. neoformans* ACKs mirrors that observed in other ASKHA superfamily members (Hurley, 1996). Enzymes with a global architecture similar to ACKs commonly employ domain closure to facilitate catalysis (for example, see (Hayward, 2004)). The ability to adopt multiple interdomain angles in the eukaryotic ACKs suggests that interdomain motions could similarly contribute to catalysis, as has been shown for the *M. thermophila* enzyme (Gorrell and Ferry, 2007).

8. Accession numbers

Coordinates and structure factors have been deposited with the RCSB Protein Data Bank with accession numbers 4H0O (*E. histolytica* ACK) and 4H0P (*C. neoformans* ACK).

Acknowledgments

This work was supported by NSF grant 0920274 (KSS), NIH grants GM084417 (KSS), GM079419 (TMI), EY018435 (TMI) and AI079558 (TMI), and Bundesministerium für Bildung und Forschung (BMBF) ZIK program grant FKZ 03Z2HN21 (MT). Use of the Advanced Photon Source was supported by the U. S. Department of Energy, Office of Science, Office of Basic Energy Sciences, under Contract No. DE-AC02-06CH11357. Use of the Life Sciences Collaborative Access Team (LS-CAT) ID21-D, and -G at Advanced Photon Source (APS) was supported by the Michigan Economic Development Corporation and the Michigan Technology Tri-Corridor for the support of this research program (Grant 085P1000817). A portion of this work used facilities that were supported by the Vanderbilt Core Grant in Vision Research (P30EY008126). This paper is Technical Contribution No. 6077

of the Clemson University Experiment Station. We thank Kathryn McCulloch, Prashant Singh, and Kendra Vann for critical reading of this manuscript.

References

Bork P, Sander C, Valencia A. An ATPase domain common to prokaryotic cell cycle proteins, sugar kinases, actin, and hsp70 heat shock proteins. Proc Natl Acad Sci USA. 1992; 89:7290–7294. [PubMed: 1323828]

Bragg PD, Reeves RE. Pathways of glucose dissimilation in Laredo strain of *Entamoeba histolytica*. Exp Parasitol. 1962; 12:393–400. [PubMed: 14014874]

Brunger AT, Adams PD, Clore GM, DeLano WL, Gros P, et al. Crystallography & NMR system: A new software suite for macromolecular structure determination. Acta Crystallogr D: Biol Crystallogr. 1998; 54:905–921. [PubMed: 9757107]

Buss KA, Ingram-Smith C, Ferry JG, Sanders DA, Hasson MS. Crystallization of acetate kinase from *Methanosarcina thermophila* and prediction of its fold. Protein Sci. 1997; 6:2659–2662. [PubMed: 9416619]

Buss KA, Cooper DR, Ingram-Smith C, Ferry JG, Sanders DA, et al. Urikinase: structure of acetate kinase, a member of the ASKHA superfamily of phosphotransferases. J Bacteriol. 2001; 183:680–686. [PubMed: 11133963]

Cowtan K. Joint CCP4 and ESF-EACBM newsletter on protein crystallography. 1994; 31:34–38.

Cozzone AJ. Regulation of acetate metabolism by protein phosphorylation in enteric bacteria. Annu Rev Microbiol. 1998; 52:127–164. [PubMed: 9891796]

Emsley P, Cowtan K. Coot: model-building tools for molecular graphics. Acta Crystallogr D: Biol Crystallogr. 2004; 60:2126–2132. [PubMed: 15572765]

Fowler ML, Ingram-Smith C, Smith KS. A novel pyrophosphate-forming acetate kinase from the protist *Entamoeba histolytica*. Eukaryot Cell. 2012 [Epub ahead of print].

Gorrell A, Ferry JG. Investigations of the acetate kinase mechanism by fluorescence quenching. Biochemistry. 2007; 46:14170–14176. [PubMed: 17999468]

Gorrell A, Lawrence SH, Ferry JG. Structural and kinetic analyses of arginine residues in the active site of the acetate kinase from *Methanosarcina thermophila*. J Biol Chem. 2005; 280:10731–10742. [PubMed: 15647264]

Hayward S. Identification of specific interactions that drive ligand-induced closure in five enzymes with classic domain movements. J Mol Biol. 2004; 339:1001–1021. [PubMed: 15165865]

Hayward S, Lee RA. Improvements in the analysis of domain motions in proteins from conformational change: DynDom version 1.50. J Mol Graph Model. 2002; 21:181–183. [PubMed: 12463636]

Hurley JH. The sugar kinase/heat shock protein 70/actin Superfamily: implications of conserved structure for mechanism. Annu Rev Biophys Biomol Struct. 1996; 25:137–162. [PubMed: 8800467]

Ingram-Smith C, Barber RD, Ferry JG. The role of histidines in the acetate kinase from *Methanosarcina thermophila*. J Biol Chem. 2000; 275:33765–33770. [PubMed: 10958794]

Ingram-Smith C, Martin SR, Smith KS. Acetate kinase: not just a bacterial enzyme. Trends Microbiol. 2006; 14:249–253. [PubMed: 16678422]

Laskowski RA, Macarthur MW, Moss DS, Thornton JM. Procheck - a program to check the stereochemical quality of protein structures. J Appl Crystallogr. 1993; 26:283–291.

McCoy AJ, Grosse-Kunstleve RW, Adams PD, Winn MD, Storoni LC, et al. Phaser crystallographic software. J Appl Crystallogr. 2007; 40:658–674. [PubMed: 19461840]

Miles RD, Iyer PP, Ferry JG. Site-directed mutational analysis of active site residues in the acetate kinase from *Methanosarcina thermophila*. J Biol Chem. 2001; 276:45059–45064. [PubMed: 11562377]

Miles RD, Gorrell A, Ferry JG. Evidence for a transition state analog, MgADP-aluminum fluoride-acetate, in acetate kinase from *Methanosarcina thermophila*. J Biol Chem. 2002; 277:22547–22552. [PubMed: 11960978]

Murshudov GN, Vagin AA, Dodson EJ. Refinement of macromolecular structures by the maximum-likelihood method. Acta Crystallogr D: Biol Crystallogr. 1997; 53:240–255. [PubMed: 15299926]

Otwinowski Z, Minor W. Processing of X-ray diffraction data collected in oscillation mode. Methods Enzymol. 1997; 276:307–326.

Reeves RE, Guthrie JD. Acetate kinase (pyrophosphate). A fourth pyrophosphate-dependent kinase from *Entamoeba histolytica*. Biochem Biophys Res Commun. 1975; 66:1389–1395. [PubMed: 172079]

Schrodinger, LLC. The PyMOL Molecular Graphics System, Version 1.3r1. 2010.

Singh-Wissmann K, Ingram-Smith C, Miles RD, Ferry JG. Identification of essential glutamates in the acetate kinase from *Methanosarcina thermophila*. J Bacteriol. 1998; 180:1129–1134. [PubMed: 9495750]

Thauer RK, Kaster AK, Seedorf H, Buckel W, Hedderich R. Methanogenic archaea: ecologically relevant differences in energy conservation. Nat Rev Microbiol. 2008; 6:579–591. [PubMed: 18587410]

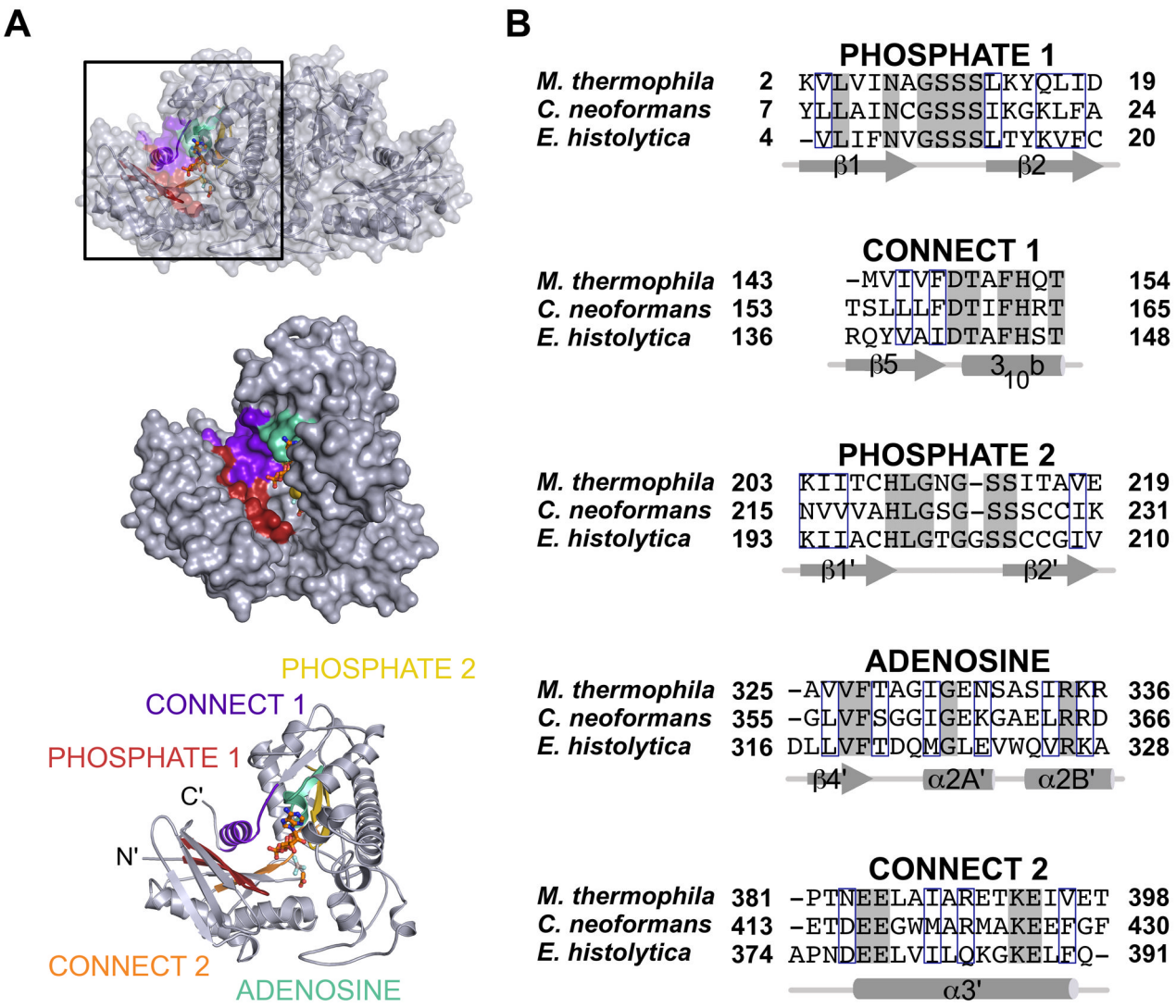

Figure 1. Conserved motifs of the ASKHA superfamily

A) Location of the ASKHA superfamily sequence motifs shown in a protomer of *C. neoformans* ACK. **B**) A structure-based sequence alignment of each motif shown with secondary structure elements labeled. Fully conserved residues are shaded grey and strongly conserved residues are outlined in blue.

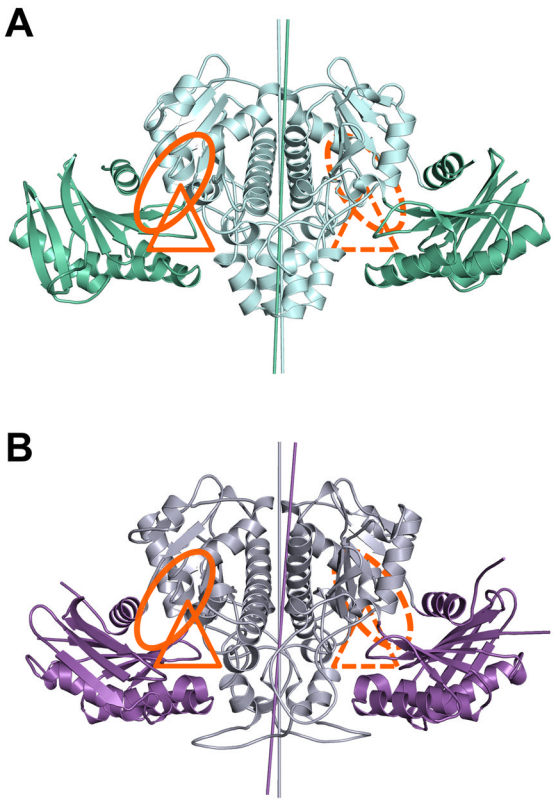

Figure 2. Structures of the eukaryotic ACKs

A) *E. histolytica* ACK with the N-terminal wing domain colored green and the C-terminal body domain colored cyan. **B**) *C. neoformans* ACK with the wing domain colored purple and the body domain colored grey. The putative acetate and nucleotide binding sites are highlighted with a triangle and a circle, respectively. The rotation axes relating each domain of the dimer are highlighted with a line colored similarly to the corresponding domain.

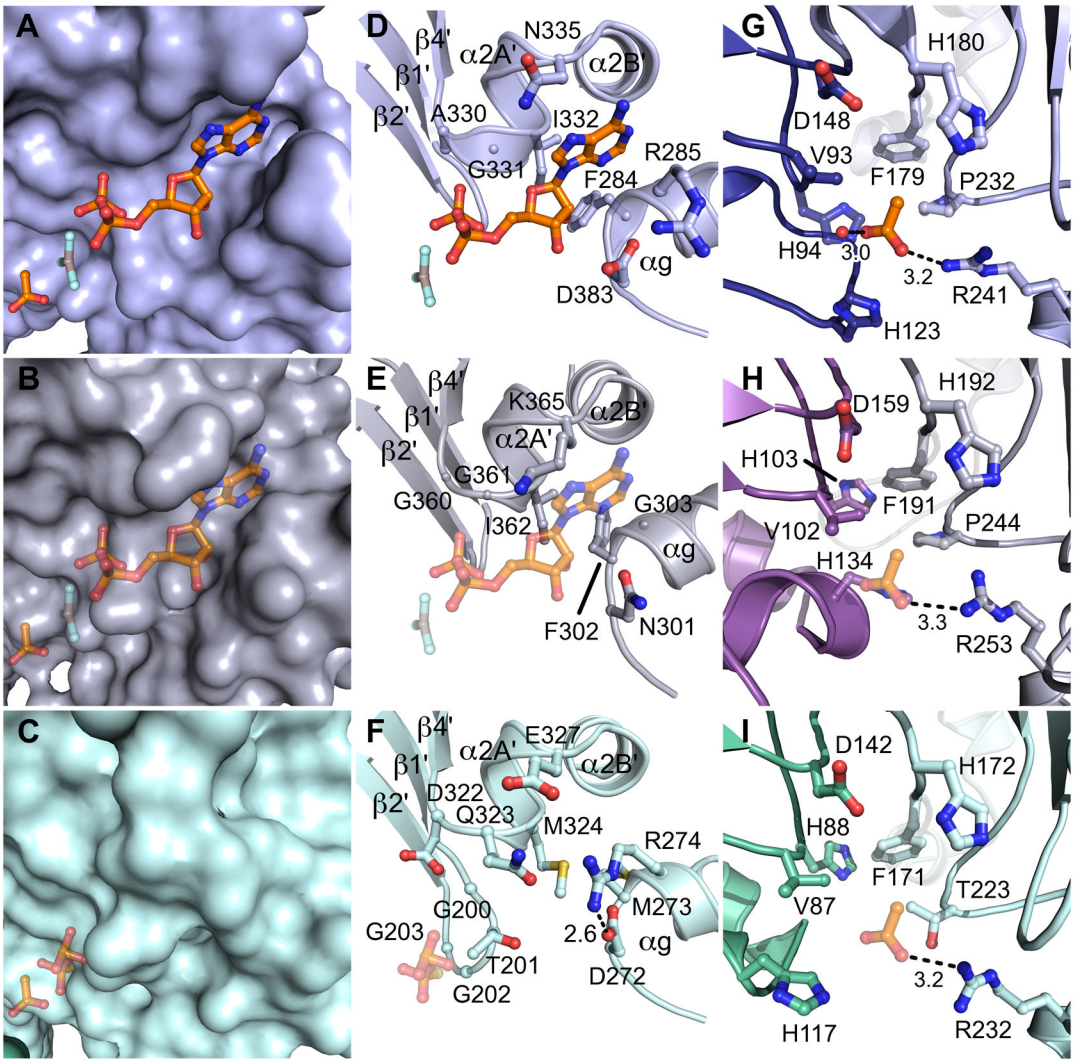

Figure 3. Active site architecture

A) A surface representation of the *M. thermophila* ACK (PDB ID 1TUY) with the N-terminal wing domain colored dark blue and the C-terminal body domain colored light blue. **B**) A surface representation of the *C. neoformans* ACK colored as in Figure 2. ADP-AlF_3 and acetate are modeled into putative binding sites. **C**) A surface representation of the *E. histolytica* ACK colored as in Figure 2 with PPS and acetate modeled into putative binding sites. **D–F**) Close up views of the nucleotide or PP_i binding sites in ACKs. **D**) *M. thermophila* ACK, **E**) *C. neoformans* ACK, and **F)** *E. histolytica* ACK. In panels **E**) and **F**), the position is modeled according to methods listed in the text. **G–I**) Close up views of the substrate binding site. **G)** *M. thermophila* ACK **H**) *C. neoformans* ACK, and **I)** *E. histolytica* ACK. The acetate is modeled in panels **H**) and **I**).

Table 1

Crystallographic data collection and refinement statistics

	***E. histolytica* ACK**	***C. neoformans* ACK**
Data collection		
APS Beamline	21-ID-G	21-ID-D
Wavelength	0.979 Å	1.127 Å
Space group	I222	$P2_1$
Unit cell dimensions	a=98.8 Å	a=51.4 Å
	b=126.9 Å	b=107.6 Å
	c=145.6 Å	c=79.1 Å
	β=90°	β=99.8°
Resolution Range	44 - 2.4 Å (2.46 - 2.4 Å)[a]	39 - 1.9 Å (1.97 - 1.9 Å)
Number of reflections	273,804	224,881
Unique reflections	35,682	64,297
R_{sym}[b]	13.8% (44.0%)	5.8% (30.9%)
$<I>/<\sigma>$[c]	15.6 (3.0)	27.0 (5.2)
Redundancy	7.7 (5.8)	3.5 (3.0)
Completeness	99.3% (93.7%)	95.7% (89.8%)
Refinement		
R_{cryst}[d]	21.0%	17.8%
R_{free}[e]	23.1%	21.9%
Rms deviation		
*B*ond Length	0.004	0.01
Bond Angle	0.93	1.2

[a] Values in parentheses are for the highest resolution shell.

[b] $R_{sym} = \Sigma_{hkl}\Sigma_j|I_j - \langle I\rangle|/\Sigma_{hkl}\Sigma I_j$ where j is the jth measurement and <I> is the weighted mean of I.

[c] $<I>/<\sigma>$ is the mean intensity divided by the mean error.

[d] $R_{cryst}=\Sigma_{hkl}||F_o| - K|F_c||/\Sigma_{hkl}|F_o|$ where F_o and F_c are the observed and calculated structure factor amplitudes, and k is a weighting factor.

[e] R_{free} is the same as R_{cryst} calculated on 5% of the reflections in *E. histolytica* ACK (1999 reflections) and *C. neoformans* ACK (3188 reflections).